Journal of Geography and Cartography 2025, 8(2), 11495.
https://doi.org/10.24294/jgc11495

Article

Enhanced statistical approach for urban groundwater flooding risk assessment

Majid Altafi Dadgar[1,2]

[1] Groundwater and Geothermal Research Center (GRC), Ferdowsi University of Mashhad, Mashhad 9177948974, Iran; Dadgarmajid77@yahoo.com
[2] Kian Madan Pars Industrial and Mining Company (KMPC), Tehran 982188623482, Iran

CITATION

Dadgar MA. Enhanced statistical approach for urban groundwater flooding risk assessment. Journal of Geography and Cartography. 2025; 8(2): 11495. https://doi.org/10.24294/jgc11495

ARTICLE INFO

Received: 10 February 2025
Accepted: 24 February 2025
Available online: 7 April 2025

Abstract: This study introduces a novel Groundwater Flooding Risk Assessment (GFRA) model to evaluate risks associated with groundwater flooding (GF), a globally significant hazard often overshadowed by surface water flooding. GFRA utilizes a conditional probability function considering critical factors, including topography, ground slope, and land use-recharge to generate a risk assessment map. Additionally, the study evaluates the return period of GF events (GFRP) by fitting annual maxima of groundwater levels to probability distribution functions (PDFs). Approximately 57% of the pilot area falls within high and critical GF risk categories, encompassing residential and recreational areas. Urban sectors in the north and east, containing private buildings, public centers, and industrial structures, exhibit high risk, while developing areas and agricultural lands show low to moderate risk. This serves as an early warning for urban development policies. The Generalized Extreme Value (GEV) distribution effectively captures groundwater level fluctuations. According to the GFRP model, about 21% of the area, predominantly in the city's northeast, has over 50% probability of GF exceedance (1 to 2-year return period). Urban outskirts show higher return values (> 10 years). The model's predictions align with recorded flood events (90% correspondence). This approach offers valuable insights into GF threats for vulnerable locations and aids proactive planning and management to enhance urban resilience and sustainability.

Keywords: extreme probability distribution functions; groundwater flooding hazard; conditional probability; rising groundwater level

1. Introduction

Groundwater flooding (GF) is a phenomenon characterized by groundwater levels exceeding normal ranges and surfacing. Despite its emergence as a global hazard with profound implications for urban infrastructure, environmental health, and socio-economic stability, GF has been historically underappreciated in hazard assessment and policy formulation. This oversight is primarily due to more visible forms of overland or riverine flooding dominating the discourse [1,2]. This oversight is particularly concerning, given the extensive damage GF can inflict, akin to traditional flooding yet characterized by distinct features and drivers. For instance, in urban areas, GF can silently undermine underground structures without visible surface manifestation, posing unique challenges for detection and management [3]. Furthermore, the deterioration of GW quality resulting from mixing with wastewater through aging and leaking sewer infrastructures endangers groundwater-related ecosystems [4].

GF's development is multifaceted, often resulting from a combination of natural and anthropogenic factors. These include heightened infiltration rates due to extreme precipitation events [5], artificial recharge, and infrastructural inadequacies, such as leaking sewer systems [4]. Moreover, changes in water resource management leading to decreased groundwater withdrawal have also been recognized as contributing factors [6,7]. Despite its global prevalence, with incidents reported in diverse regions, including the UK and the US [1,8,9], GF remains inadequately represented in risk maps and management strategies. This gap is highlighted by the European Union's Flood Directive (2007/60/EC), which mandates GF risk mapping yet faces challenges due to methodological limitations and data scarcity [10]. Identifying areas susceptible to GF is crucial, establishing a foundation for decision makers to address critical issues. Groundwater flooding risk maps are recommended to illustrate potential adverse consequences [10].

Current GF risk mapping techniques, encompassing stochastic and numerical models, machine learning, and analytical approaches [11–15], face obstacles due to insufficient comprehension of local geological and hydrological conditions, variability in GF causes, and challenges in model calibration arising from data paucity [16,17].

To address these critical gaps, this study proposes a novel GF risk mapping approach based on conditional probability. We introduce an innovative methodology that integrates several probability distribution functions (PDFs) to estimate the return period of GF events using historical data on annual maximum groundwater levels. This approach is validated through a case study in a southeastern Iranian urban aquifer with recorded GF incidents, offering insights into the methodology's effectiveness and wider applicability. By advancing our understanding of GF dynamics and providing a robust assessment tool, this research not only contributes to the scientific discourse but also carries substantial implications for urban planning, disaster management, and global climate change adaptation strategies. It is important to note that the risk associated with groundwater flooding is a combination of hazard, vulnerability, and exposure and this study primarily focuses on the hazard component and its contributing factors.

2. Materials and methods

2.1. Study area

Behbahan city in southeastern Khuzestan province, Iran, serves as a compelling case study for examining GF dynamics due to its distinct hydrogeological features and heightened susceptibility to GF hazards. With a population of approximately 120,000 inhabitants, this urban area is situated in a critical zone of the aquifer, characterized by shallow depths that predispose it to frequent GF events. The study area, encompassing approximately 142 km^2, lies in the aquifer's lowest part, rendering it particularly vulnerable to hydrological changes. Geographically, it spans from 30°32′31″ N to 30°39′46″ N latitude and from 50°11′29″ E to 50°18′30″ E longitude, as illustrated in **Figure 1**, which also depicts groundwater flow and contour lines.

Several factors contribute to the area's GF risk. The city's inadequate drainage system, proximity to gaining rivers, fine-grained surface soils, and extensive irrigation networks lead to a shallow aquifer, particularly within the 30 km^2 urban-covered area. Situated at an altitude of 21.38 m above sea level, Behbahan exhibits a subtropical climate. According to Ehya and Marbouti [18], the region's average annual temperature is around 30 ℃, with an annual precipitation of approximately 336 mm.

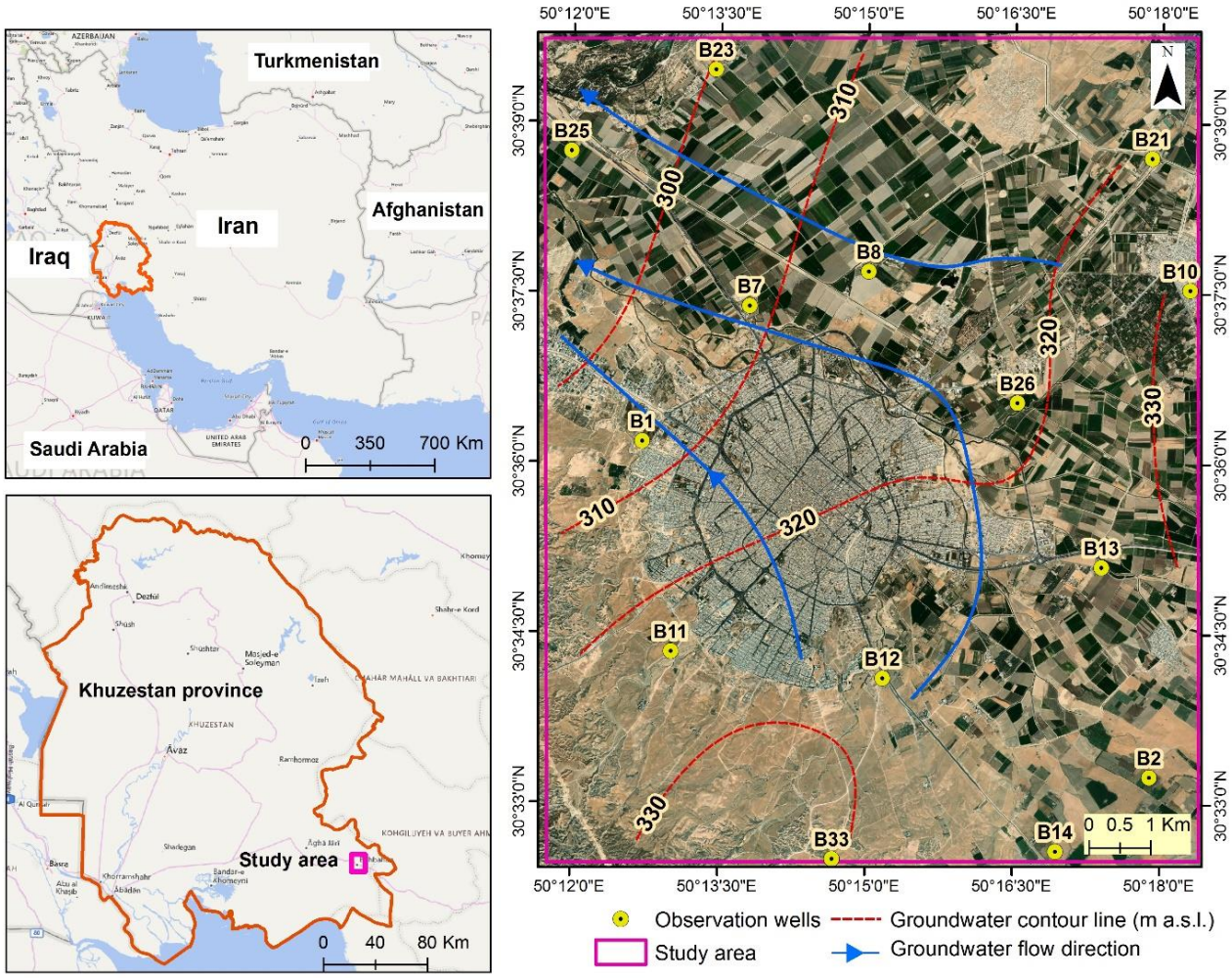

Figure 1. Location map of the study area, illustrating groundwater flow patterns and contour lines.

Hydrogeologically, the aquifer has an average thickness of approximately 50 m within the study scope. Groundwater depth varies across the area, with central regions exhibiting shallower depths compared to the southern parts. The general groundwater flow originates from the southern and eastern parts, moving towards the northwestern parts, aligning with the Maroon River's discharge (**Figure 1**). The highland geological units, ranging from upper cretaceous carbonate and evaporite rocks to more recent conglomerate and alluvial deposits, provide the aquifer materials through erosion processes. The surface soil is primarily composed of finely graded materials like marl, clay, and silty clay, characterized by their low hydraulic conductivity and substantial water-retention capabilities. The extensive irrigation

networks, drawing water primarily from surface resources, substantially contribute to aquifer recharge, in addition to precipitation and lateral flow sources.

This detailed characterization of Behbahan city not only underscores its vulnerability to GF but also highlights its representativeness for studying GF phenomena in similar subtropical urban settings. The combination of climatic, hydrological, and geological factors renders this area an ideal model for the development and evaluation of novel GF risk assessment methodologies. The knowledge gained from this study holds potential implications for global urban centers worldwide that face similar challenges.

2.2. Groundwater monitoring

In this study, we employed a comprehensive groundwater monitoring network within Behbahan city, comprising 14 observation wells with data spanning from 2002 to 2022. This dataset, characterized by its monthly temporal resolution, provides a valuable long-term perspective on aquifer dynamics. Historical analysis uncovers periods of significant tension within the aquifer, notably from 2006 to 2009 and 2013 to 2017. These periods were primarily influenced by excessive groundwater extraction and decreased precipitation. These fluctuations ranged from 315.7 to 319 m.a.s.l., are depicted in **Figure 2**. Notably, years with precipitation surpassing the 336 mm/year average corresponded with a rise in groundwater levels (**Figure 2**), highlighting the direct impact of climatological variables on aquifer behavior. This relationship is further evidenced by the reduced pumping rates and stabilized groundwater levels during years of higher-than-average precipitation, such as 2003, 2013, and 2017, in contrast to the significant fluctuations observed during drier years like 2006, 2007, 2009, and 2014.

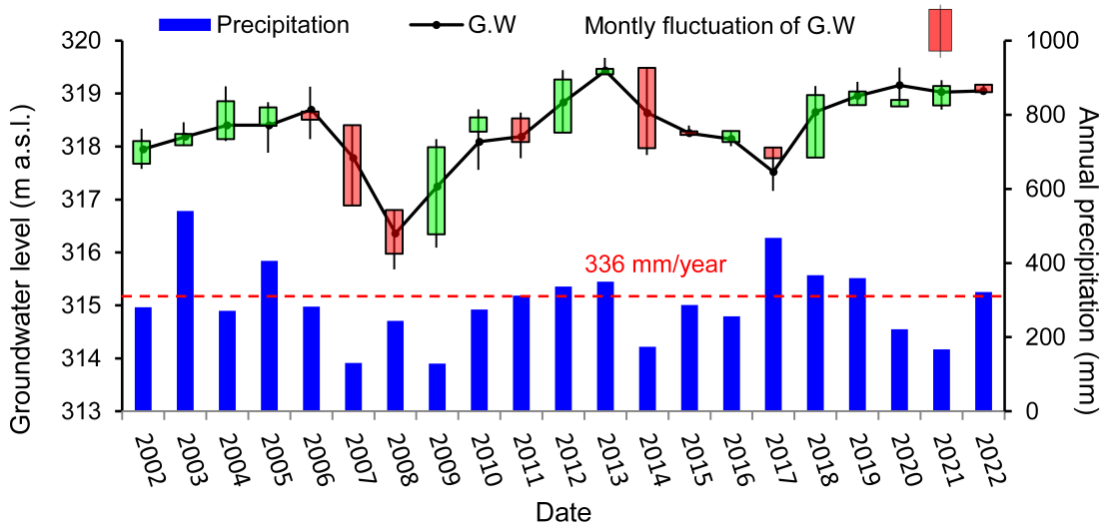

Figure 2. Monthly groundwater level fluctuations (green and red boxes), average annual groundwater fluctuations (black line), annual precipitation (blue bar), and average annual precipitation (red-dashed line).

2.3. Groundwater flooding

Since 2013, Behbahan city has intermittently encountered groundwater flooding; a phenomenon influenced by both physical factors and management

practices. Contributing factors include the city's low-permeability surface soil, inadequate drainage systems, and its location within the aquifer's low-lying areas. Furthermore, the management of aquifer withdrawals during various climatic conditions has a crucial impact on the occurrence of GF. A field survey conducted in 2019 documented 40 instances of GF, affecting both open areas and building basements (**Figure 3**). This survey provided valuable insights into the environmental conditions and geographical distribution of GF incidents.

Figure 3. Geographical distribution of reported groundwater flooding incidents, and the types of affected structures: **(a)** Foundation; **(b)** shopping center; **(c)** basement; **(d)** building's yard.

2.4. Maps for groundwater flooding risk assessment

To generate a comprehensive Groundwater Flooding Risk Assessment (GFRA), this study employed three key driving factors: A digital elevation map, a slope map, and a land use-recharge map. The digital terrain model (DTM) was derived by processing over 10,000 elevation data points from the National Cartographical Center of Iran and refining them through a digital surface model (DSM) sourced from earthexplorer.usgs.gov [19]. The resulting DTM was further categorized into five distinct elevation classes using ArcGIS, as illustrated in **Figure 4**. Topographical changes can pose crucial effects on the timing and extent of GF [3]. The slope map, obtained from the processed DSM, reveals that the majority (65%) of the area falls within a 0%–1.15% slope class. This observation suggests that the most

critical groundwater mounds are more likely to develop in the low-slope areas of aquifers [1].

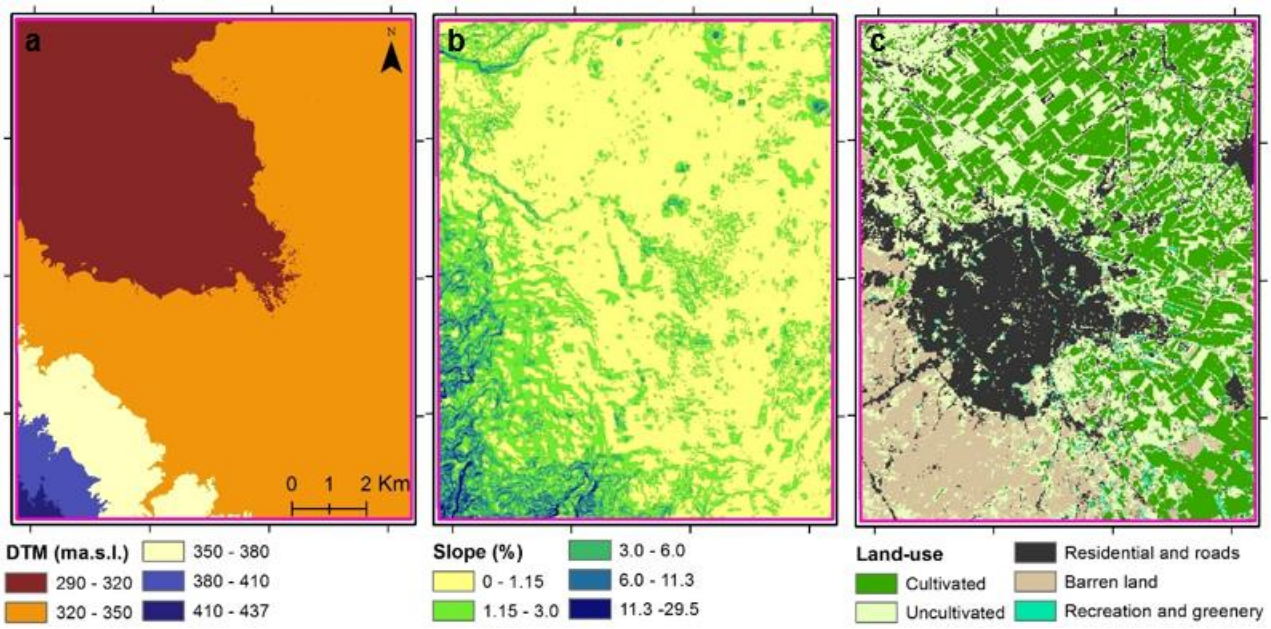

Figure 4. (a) Digital terrain model; **(b)** slope map; **(c)** land-use map of the study area.

The land-use map, sourced from Landsat 8 satellite imagery, was analyzed to classify five primary land-use types within the region. This map played a pivotal role in delineating distinct recharge zones, which are critical in generating the GFRA. The region exhibits mixed land use, including residential areas ~20.5%, barren and uncultivated areas ~47%, cultivated areas ~31%, and recreation and greenery areas ~1.5%. The recharge assumptions, adapted from the studies by Dadgar et al. [20,21], were integrated to account for the impacts of different land uses on groundwater recharge. In residential areas, where impervious surfaces have largely replaced natural terrain, recharge was considered negligible. This assumption is consistent with the findings of Nguyen et al. [22], who suggest that in urbanized settings, the proximity of groundwater levels to the surface reduces the possibility of wastewater system exfiltration contributing to groundwater recharge. It should be noted that the quantity of recharge was not explicitly incorporated into the calculations, but rather employed to illustrate the impacts of recharged and non-recharged regions on the probability of the GF risk. To facilitate the analysis, a unique code was assigned to each class of driving factors, ranging from 1 to 5. For instance, code 1 corresponds to class "290–320" in the DTM, class "0–1.15" in the slope category, and class "Cultivated" in land-use classification. This coding system was applied consistently across all driving factors to streamline the evaluation process.

2.5. Probability function and frequency risk

The methodology of this study, as illustrated in **Figure 5**, revolves around the application of a conditional probability function. This approach premised on the principle that the occurrence of certain events can be contingent on others [23], is particularly apt for analyzing complex environmental systems such as groundwater

flooding. The conditional probability equation employed in this study can be expressed as follows:

$$P(B/A) = \frac{P(B \cap A)}{P(A)} \quad (1)$$

where $P(B/A)$ represents the probability of event B given that event A has already occurred. This equation forms the backbone of our analysis, where three independent variables—ground elevation, ground slope, and recharge zones—are considered as antecedent events, and the depth to the groundwater table is treated as the dependent variable. A critical depth cut-off of 10 m was established, taking into account the distinct soil characteristics of the study area, which allow water uptake from the water table up to this depth. Hence, observation wells that did not meet this criterion were excluded from further investigation.

The Frequency Risk (FR) index was derived by first calculating the success percentages of conditional probabilities for each factor and then averaging and normalizing these values to create an index ranging from 0 to 1. Building upon similar methodologies employed in previous studies [e.g., 15,24], we categorized the FR into five risk classes: No Risk (FR = 0), Low (0 < FR < 0.5), Medium (0.5 < FR < 0.7), High (0.7 < FR < 0.9), and Critical (0.9 < FR ≤ 1). This classification system allows for a more nuanced understanding of the varying levels of susceptibility to groundwater flooding, enabling decision-makers to prioritize resources and mitigation efforts accordingly. The thresholds for each risk class were carefully selected to balance sensitivity and specificity in identifying areas at risk, while also accounting for potential uncertainties in the underlying data and methodologies.

The process for generating the GFRA comprises the following steps:

- Creation of thematic maps for all variables, ensuring a consistent pixel size, and classification of the independent variables into four or five distinct classes.
- Calculation of the probability for each factor by determining the number of pixels in each class and subsequently normalizing these values.
- Assessment of the intersection between dependent and independent factors to determine the success percentage.
- Application of the conditional probability equation to calculate the probability of the dependent factor.

In order to combine the impacts of three independent factors into a single representative risk map, the conditional probabilities associated with each independent factor were averaged within each pixel. The resulting value for each pixel was normalized to generate a novel classification for groundwater flooding risks. This GFRA was subsequently validated against field survey data, confirming the model's precision in identifying actual flooded locations.

2.6. Probability distribution functions and map for groundwater flooding return period

Frequency analysis, a fundamental technique in hydrological studies [25], was employed to analyze the behavior of the groundwater system using historical data fitting methods. This study's exploration into the return period of groundwater

flooding events represents a significant advancement in hydrogeological risk assessment. Drawing from the findings of Guerriero et al. [26], we acknowledged the hydrogeological heterogeneity of large areas by employing multiple probability models. This approach recognizes the diverse hydrological responses across different observation wells due to the unique tensions imposed on the aquifer. Hence, various PDFs were considered to fit the annual maxima time series of groundwater levels, including Weibull, Fréchet, Gumbel, and the Generalized Extreme Value (GEV) distribution [27]. The selection and application of these PDFs are detailed in the Appendix. To ensure the most accurate representation of the data, the performance of each PDF was evaluated using goodness-of-fit tests, such as the Anderson-Darling (AD), Kolmogorov-Smirnov (KS), and Chi-Squared (x^2) tests [28]. This analysis was conducted using the EasyFit tool. Consequently, the most appropriate distribution was used to predict the return periods of groundwater levels, culminating in the creation of a Groundwater Flooding Return Period (GFRP) map.

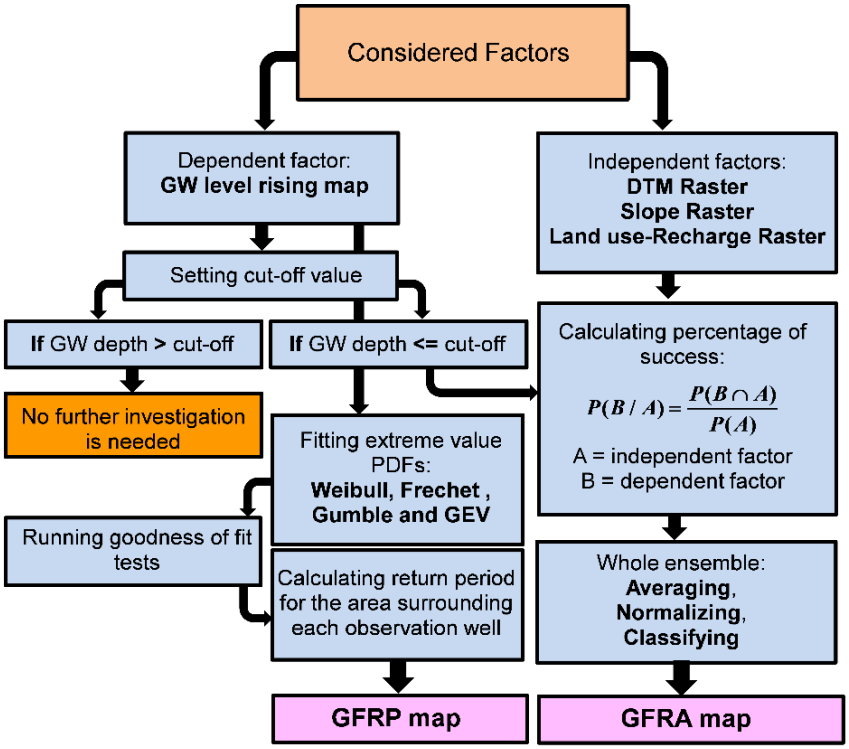

Figure 5. Flowchart illustrating the proposed framework for generating the GFRA and the GFRP.

3. Results and discussion

3.1. Frequency risk

The analysis of frequency risk in relation to driving factors confirms the crucial role of topographical features in GF incidents. As **Figure 6a** shows GF mostly occurs in low-lying areas, indicating the groundwater table is mainly susceptible to rising in lowland areas [4]. Almost 100% of the critical-risk zone lies within the 290–320 m elevation range, while this range concurrently exhibits the least percentage of no-risk areas. Regions with elevations higher than 350 m appear to be

exempt from GF risk, which can be considered in future urban development. Groundwater flow is normally governed by ground slope, with gentler slopes being more susceptible to groundwater mounding. **Figure 6b** corroborates this, in which most GF incidents occur on slopes lower than 3%. In this case, areas with slopes steeper than 11% can be considered without GF risk. The high- and critical-risk zones are predominantly located within the first two slope classes, where covered by residential areas (see **Figure 6c**). Almost 40% of urban areas fall within high- and critical-risk levels, highlighting a critical finding. Despite the absence of recharge as a contributing factor in these urban areas, their low elevation and flat topography substantially increase their susceptibility to groundwater flooding. Recreational regions exhibit a 20% frequency risk, characterized by high and critical risk levels. The results of the frequency risk analysis suggest that the southeastern part of the region can be considered for future urban development planning, as it offers opportunities for expansion while mitigating potential groundwater flooding risks.

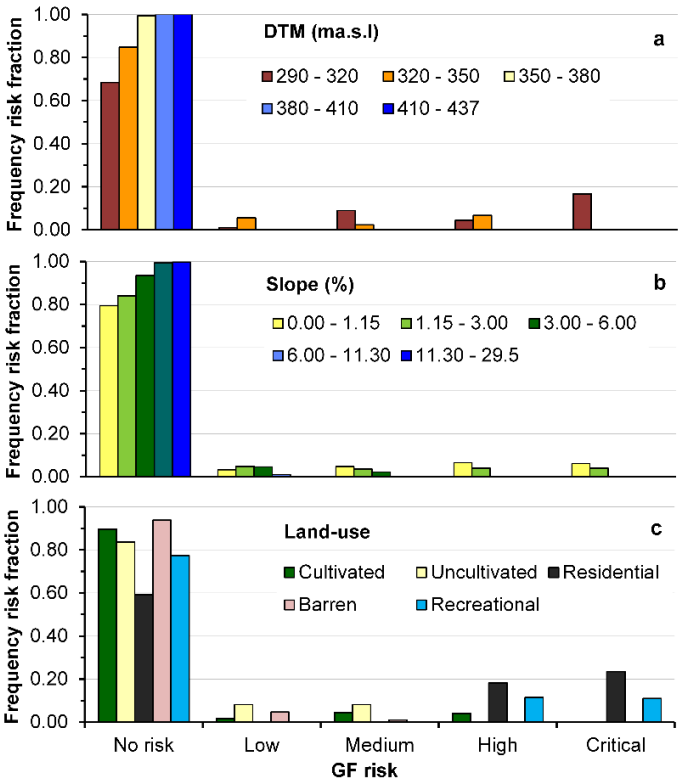

Figure 6. Frequency risk of groundwater flooding regarding driving factors: **(a)** DTM; **(b)** slope; **(c)** land-use.

3.2. Groundwater flooding risk assessment (GFRA)

The GFRA map generated in this study represents a significant advancement in assessing spatial groundwater flooding risks. As illustrated in **Figure 7a**, the GFRA uncovers a critical level of risk in the central, northern, and eastern parts of the city. This is further corroborated by the GFRA, which identifies specific regions in the southeast and northwest as exhibiting low to high risk levels, underscoring the need for careful consideration in future urban planning and development (**Figure 7c**). The urban developed area, as shown in **Figure 7d**, displays a medium to high level of

risk, aligning with the findings of Chebanov and Zadniprovska [24], Allocca et al. [15]. Our approach offers several methodological advantages over earlier studies. It leverages commonly available hydrogeological data, such as groundwater level monitoring and recharge zone maps, circumventing the need for extensive field data on soil properties and hydraulic characteristics. This aspect is particularly advantageous in regions where such data are scarce or difficult to obtain. The model's validation, as depicted in **Figure 7b**, demonstrates a robust correlation between predicted and recorded groundwater flooding points. The majority of recorded GF incidents are located within the critical risk zone, while the remaining incidents, except for one, fall within the high-risk zone. This notable correspondence validates the efficacy of our model and underscores its practical applicability in real-world scenarios. Furthermore, the approach's reduced reliance on extensive data sets for calibration distinguishes it from other models that necessitate substantial data inputs. This aspect is particularly relevant in the context of developing regions or areas with limited monitoring infrastructure. Our findings resonate with the work of Coda et al. [17], who also employed a probability modeling approach, reinforcing the potential of such methodologies in Groundwater Flooding Risk Assessment.

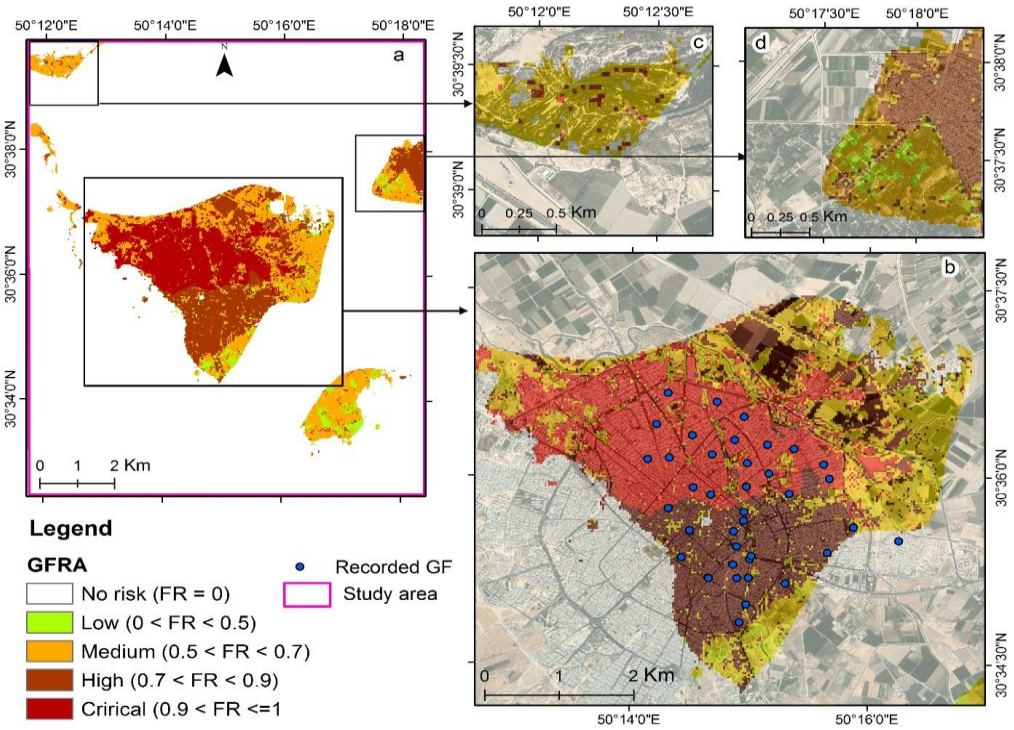

Figure 7. Groundwater flooding risk assessment (GFRA) map of the **(a)** study area; **(b)** comparison of GFRA and recorded flooding points; **(c)** GFRA in relation to urban area development; **(d)** GFRA in relation to the developed area.

3.3. Groundwater flooding return period (GFRP)

This section discusses the results of fitting probability density functions and evaluating their goodness of fit. Analyzing goodness of fit is crucial to understand which distribution best represents the observed patterns within the samples. In contrast to surface water studies, where the GEV distribution has been extensively explored, our research pioneers the evaluation of various extreme continuous

distributions for groundwater levels. This novel approach not only aids in generating a GFRA map but also paves the way for estimating groundwater flood return periods. Our analysis focused on fitting various PDFs to groundwater level data and rigorously assessing their goodness of fit. This crucial process of identifying the most accurate distribution model is illustrated in **Figure 8**. The GEV distribution emerged as the superior model, demonstrating the highest fit and lowest rejection rates (**Table 1**). The Weibull model ranked second in terms of fit, while the Frechet model showed the least suitability regarding the numbers of rejections. Notably, the Chi-squared test seldom rejected the GEV distribution, suggesting its robustness in modeling extreme groundwater levels, despite the sample size limitations highlighted by Cunnane [25]. The flexibility of the GEV distribution, which allows it to encompass the Gumbel, Frechet, and Weibull distributions, is particularly advantageous for capturing extreme groundwater levels. This adaptability is further supported by the negative average value of the shape parameter, k (−0.355), in our dataset (**Table 1**). Such a characteristic reflects an unbounded distribution, which is desirable for practical applications as it allows for the modeling of larger return periods [28]. According to the statistics from **Table 1**, the GEV distribution function was selected to estimate the probability of groundwater level exceedance, and subsequently return periods were estimated.

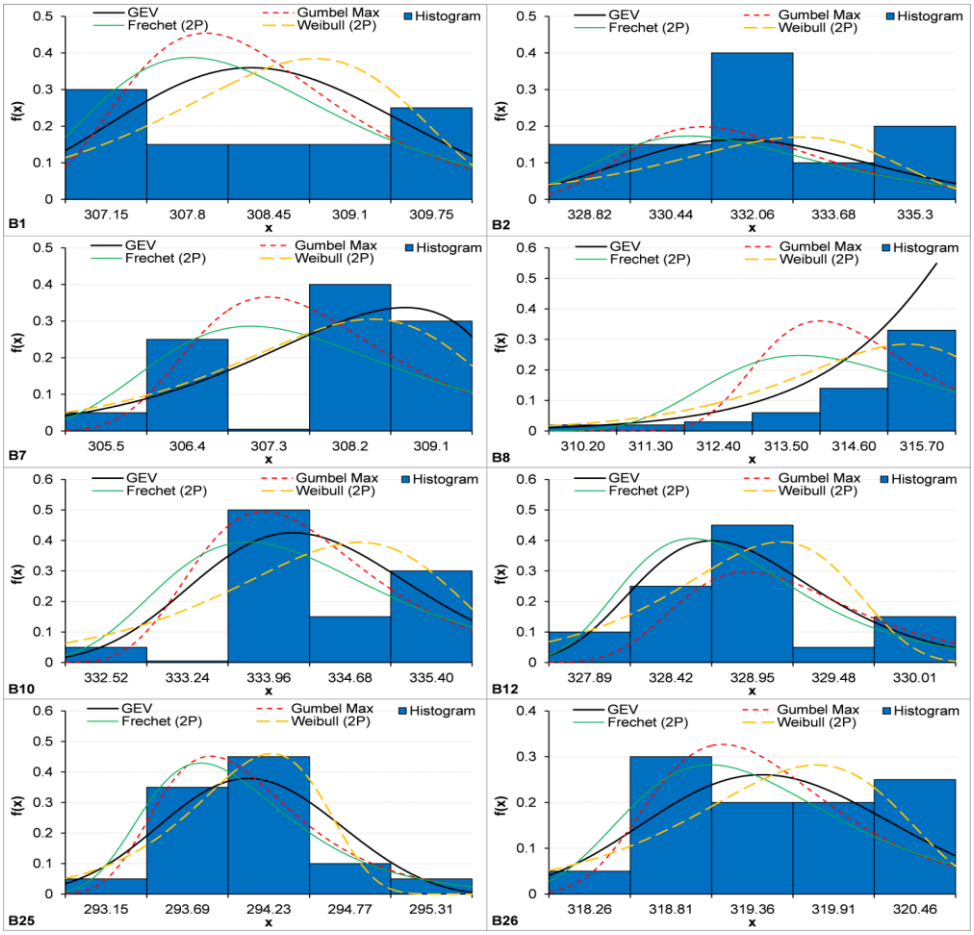

Figure 8. Graphical representation of fitted PDFs for maximum groundwater level data in each observation well. The $f(x)$ axis and x-axis stand for the probability of occurrence and the maxima groundwater level distributions, respectively.

Table 1. Statistics for the fitted PDFs and goodness of fit analysis.

Observation well	Distribution	Parameters†	Goodness of Fit (rank/rejection)		
			AD	**KS**	x^2
B1	Frechet (2P)	α = 323.42, β = 307.51	3/No	2/No	3/1
	Gen. Extreme Value	k = −0.24975, σ = 1.0599, μ = 307.69	2/No	1/No	2/No
	Gumble Max	σ = 0.81136, μ = 307.62	4/No	4/No	4/2
	Weibull (2P)	α = 322.09, β = 308.5	1/No	3/No	1/No
B2	Frechet (2P)	α = 155.31, β = 330.03	4/No	2/No	2/No
	Gen. Extreme Value	k = −0.21397, σ = 2.3114, μ = 330.43	1/No	1/No	4/3
	Gumble Max	σ = 1.8567, μ = 330.28	2/No	3/No	1/No
	Weibull (2P)	α = 227.04, $\beta = 4.7676 \times 10^{-4}$, γ =5.6949	3/No	4/No	3/No
B7	Frechet (2P)	α = 238.46, β = 306.59	4/2	3/No	1/No
	Gen. Extreme Value	k = −0.65326, σ = 1.4534, μ = 307.12	1/No	1/No	2/No
	Gumble Max	σ = 1.006, μ = 306.77	3/2	4/2	4/2
	Weibull (2P)	α = 255.55, β = 307.89	2/No	2/No	3/No
B8	Frechet (2P)	α = 210.49, β = 312.52	4/3	3/2	4/3
	Gen. Extreme Value	k = −0.96169, σ = 1.3408, μ = 313.35	1/No	1/No	2/No
	Gumble Max	σ = 1.0203, μ = 312.78	3/1	4/3	3/No
	Weibull (2P)	α = 242.74, β = 313.97	2/No	2/No	1/No
B10	Frechet (2P)	α = 357.7, β = 333.4	4/2	3/1	4/1
	Gen. Extreme Value	k = −0.19836, σ = 0.88432, μ = 333.6	3/No	2/No	1/No
	Gumble Max	σ = 0.74364, μ = 333.53	2/1	4/1	2/No
	Weibull (2P)	α = 357.81, β = 334.37	1/No	1/No	3/No
B12	Frechet (2P)	α = 604.37, β = 328.29	4/No	3/No	2/No
	Gen. Extreme Value	k = −0.08685, σ = 0.55573, μ =328.36	2/No	1/No	3/No
	Gumble Max	σ = 0.50098, μ = 328.35	1/No	2/No	1/No
	Weibull (2P)	α = 588.56, β = 328.86	3/No	4/1	4/No
B25	Frechet (2P)	α = 627.79, β = 293.51	4/No	3/No	1/No
	Gen. Extreme Value	k = −0.29376, σ = 0.55589, μ = 293.64	1/No	1/No	4/No
	Gumble Max	σ = 0.44417, μ = 293.57	3/No	2/No	2/No
	Weibull (2P)	α = 673.75, β = 293.98	2/No	4/1	3/No
B26	Frechet (2P)	α = 458.8, β = 318.81	3/No	2/No	3/No
	Gen. Extreme Value	k = −0.24832, σ = 0.77859, μ = 318.95	1/No	1/No	2/No
	Gumble Max	σ =0.60015, μ = 318.89	4/No	3/No	4/No
	Weibull (2P)	α = 459.31, β = 319.54	2/No	4/No	1/No
Total	Frechet (2P)	-	4/7	2/3	3/5
	Gen. Extreme Value	-	1/No	1/No	2/3
	Gumble Max	-	3/4	4/6	4/4
	Weibull (2P)	-	2/No	3/2	1/No

† α and β are the Frechet's shape and scale parameters, k, σ and μ are the GEV's shape, scale, location parameters, σ and μ are scale and location parameters of the Gumble Max distribution, and for the Weibull, α and β stand for shape and scale parameters, respectively.

The final GFRP map, depicted in **Figure 9**, reveals significant spatial variability in flooding risk. The northern part of the study area shows a high likelihood of groundwater flooding, with a return period of less than 2 years. In contrast, the central and northeastern urban regions exhibit a 20% probability of exceedance. This map is an invaluable resource for urban planning and risk management, offering crucial insights into areas prone to recurrent groundwater flooding. As a preemptive tool, it highlights regions where residential expansion might exacerbate flooding risks.

The validation of the GFRP map, however, presented challenges due to the lack of historical data on groundwater flooding events. We relied on visual evidence, survey data, and local testimonies to corroborate our model's predictions. Comparing **Figures 7b** and **9b** shows a strong correspondence between survey data and areas predicted to encounter more frequent flooding, particularly in regions with return periods of less than 5 years. This correlation reinforces the model's reliability, as 90% of survey data aligns with areas characterized by return periods of less than 5 years.

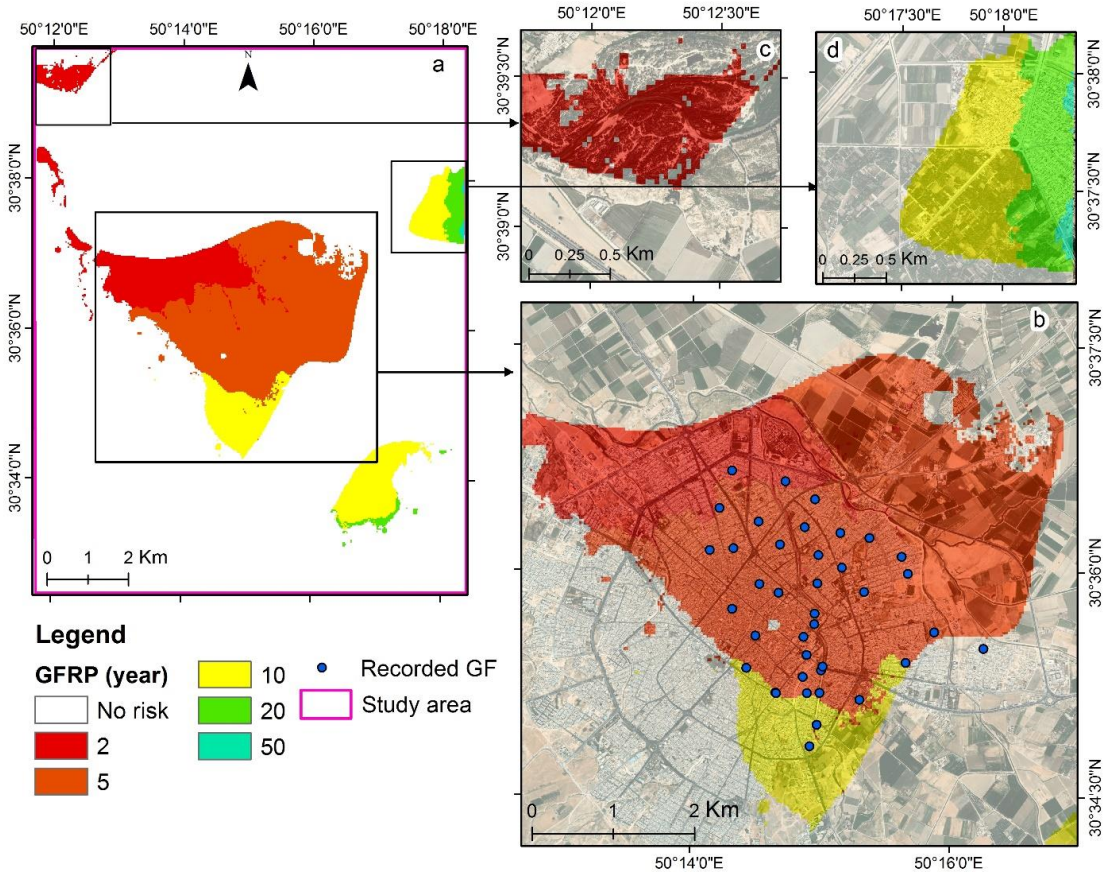

Figure 9. Groundwater flood return period (GFRP) map of **(a)** study area; **(b)** Behbahan city; **(c)** groundwater drainage area; **(d)** urban developed area.

3.4. Integrated impact and implications

The integration of GFRA and GFRP analyses in this study provides a comprehensive framework for understanding and managing groundwater flooding risks in urban environments. This approach, leveraging conditional probability

functions and probability distribution models, offers significant insights for urban planning, policy formulation, and environmental management.

The study's findings emphasize the critical role of topography and slope variations in influencing groundwater flooding, suggesting that water accumulation in high recharge areas gradually moves towards lower topographic lands due to ground slope. This has profound implications for urban development and flood mitigation strategies, highlighting the need to account for these factors in urban planning processes [29,30]. The proposed classification system for GFRA, including No Risk, Low, Medium, High, and Critical risk categories, effectively delineates areas susceptible to groundwater flooding. The model's high accuracy, as evidenced by its alignment with 91% of recorded flood events, demonstrates its practical utility in predicting flood-prone areas. This is particularly valuable for urban planners and policymakers in making well-informed decisions regarding infrastructure development and emergency preparedness measures. Furthermore, the application of various probability distribution functions, particularly the Generalized Extreme Value (GEV) distribution, facilitates a nuanced understanding of groundwater level fluctuations and flooding return periods. This approach is essential for predicting the frequency of flooding events and formulating targeted flood mitigation strategies [31–33]. The study's methodology, which employs commonly available hydrogeological data, offers a practical and accessible means of assessing groundwater flooding risks. This is especially beneficial for regions with limited data availability, as it reduces reliance on extensive field data. The validation of the GFRP using visual evidence, survey data, and local knowledge further strengthens the model's credibility.

In summary, this integrated analysis of groundwater flooding risk and return period provides actionable insights for mitigating the impacts of groundwater flooding on society and the environment. The study not only contributes to the scientific understanding of groundwater flooding dynamics but also delivers practical strategies for enhancing urban resilience, informing policy development, and promoting environmental sustainability. The methodologies and findings of this research hold the potential to be applied in other urban areas facing similar groundwater flooding challenges, rendering it a valuable contribution to the field of hydrology and urban planning [34,35].

4. Conclusion

This study introduces a novel methodology for assessing the susceptibility of urban areas to groundwater flooding risk by employing a conditional probability function to generate the Groundwater Flooding Risk Assessment (GFRA) and utilizing a range of continuous extreme probability density functions to estimate the return period of groundwater flooding events. The key findings of this investigation are as follows:

1) Topographical influence on groundwater flooding: The study reveals that topography and slope variations significantly influence groundwater flooding incidence. This suggests that water ponding in areas with high recharge rates

gradually moves towards lower topographic lands due to ground slope, despite the slow movement of groundwater.

2) Classification system and GFRA performance: The proposed classification system, comprising No Risk, Low, Medium, High, and Critical risk categories based on the Frequency Risk index, effectively delineates areas susceptible to groundwater flooding. The GFRA's performance was validated against field survey data, with only one out of 40 observed sites falling outside the projected boundary. This high level of accuracy underscores the model's practicality in predicting flood-prone areas.
3) Goodness of fit and return period analysis: The goodness of fit tests indicated that the Generalized Extreme Value (GEV) distribution provided the best fit in most cases, although the Gumbel and Weibull distributions were also suitable in certain scenarios. This highlights the need to test different PDFs in aquifers with heterogeneities.

The generation of the GFRA and GFRP maps provides decision-makers and local authorities with valuable tools for understanding groundwater flooding threats, visualizing vulnerable areas, and issuing early warnings for urban development planning.

However, the effectiveness of this approach in other case studies remains to be established. Further investigations in diverse urban settings are required to validate the adaptability and robustness of this methodology and explore its potential widespread application in Groundwater Flooding Risk Assessment.

Funding: The research was funded by the Ferdowsi University of Mashhad (RGPIN-2022-05017).

Acknowledgments: The research was funded by the Ferdowsi University of Mashhad (RGPIN-2022-05017). I am extremely grateful for the financial support provided by the university. I would also like to express my sincere gratitude to Asim Biswas for his valuable insights and comments that have significantly enriched the quality of this research.

Institutional review board statement: No applicable.

Informed consent statement: No applicable.

Conflict of interest: The author declares no conflict of interest.

References

1. Hughes AG, Vounaki T, Peach DW, et al. Flood risk from groundwater: examples from a Chalk catchment in southern England. Journal of Flood Risk Management. 2011; 4(3): 143-155. doi: 10.1111/j.1753-318x.2011.01095.x
2. Abboud JM, Ryan MC, Osborn GD. Groundwater flooding in a river-connected alluvial aquifer. Journal of Flood Risk Management. 2018; 11(4). doi: 10.1111/jfr3.12334
3. Macdonald D, Dixon A, Newell A, et al. Groundwater flooding within an urbanised flood plain. Journal of Flood Risk Management. 2011; 5(1): 68-80. doi: 10.1111/j.1753-318x.2011.01127.x
4. Al-Sefry SA, Şen Z. Groundwater Rise Problem and Risk Evaluation in Major Cities of Arid Lands – Jedddah Case in Kingdom of Saudi Arabia. Water Resources Management. 2006; 20(1): 91-108. doi: 10.1007/s11269-006-4636-2
5. Mancini CP, Lollai S, Volpi E, et al. Flood Modeling and Groundwater Flooding in Urbanized Reclamation Areas: The Case of Rome (Italy). Water. 2020; 12(7): 2030. doi: 10.3390/w12072030

6. Kreibich H, Thieken AH. Assessment of damage caused by high groundwater inundation. Water Resources Research. 2008; 44(9). doi: 10.1029/2007wr006621
7. Mohammadzadeh H, Dadgar MA, Nassery H. Prediction of the effect of water supplying from Shirindare dam on the Bojnourd aquifer using MODFLOW2000. Water Resources. 2017; 44(2): 216-225. doi: 10.1134/s009780781702004x
8. Gotkowitz MB, Attig JW, McDermott T. Groundwater flood of a river terrace in southwest Wisconsin, USA (Portuguese). Hydrogeology Journal. 2014; 22(6): 1421-1432. doi: 10.1007/s10040-014-1129-x
9. Jerome Morrissey P, McCormack T, Naughton O, et al. Modelling groundwater flooding in a lowland karst catchment. Journal of Hydrology. 2020; 580: 124361. doi: 10.1016/j.jhydrol.2019.124361
10. European Union Directive. Directive 2004/18/EC of the European Parliament and of the council on the assessment and management of flood risks. Official Journal of the European Union; 2007.
11. Sommer T, Karpf C, Ettrich N, et al. Coupled modelling of subsurface water flux for an integrated flood risk management. Natural Hazards and Earth System Sciences. 2009; 9(4): 1277-1290. doi: 10.5194/nhess-9-1277-2009
12. Fürst J, Bichler A, Konecny F. Regional Frequency Analysis of Extreme Groundwater Levels. Groundwater. 2014; 53(3): 414-423. doi: 10.1111/gwat.12223
13. Habel S, Fletcher CH, Rotzoll K, et al. Development of a model to simulate groundwater inundation induced by sea-level rise and high tides in Honolulu, Hawaii. Water Research. 2017; 114: 122-134. doi: 10.1016/j.watres.2017.02.035
14. Colombo L, Gattinoni P, Scesi L. Stochastic modelling of groundwater flow for hazard assessment along the underground infrastructures in Milan (northern Italy). Tunnelling and Underground Space Technology. 2018; 79: 110-120. doi: 10.1016/j.tust.2018.05.007
15. Allocca V, Di Napoli M, Coda S, et al. A novel methodology for Groundwater Flooding Susceptibility assessment through Machine Learning techniques in a mixed-land use aquifer. Science of The Total Environment. 2021; 790: 148067. doi: 10.1016/j.scitotenv.2021.148067
16. Naughton O, Johnston PM, McCormack T, et al. Groundwater flood risk mapping and management: examples from a lowland karst catchment in Ireland. Journal of Flood Risk Management. 2015; 10(1): 53-64. doi: 10.1111/jfr3.12145
17. Coda S, Tufano R, Calcaterra D, et al. Groundwater flooding hazard assessment in a semi-urban aquifer through probability modelling of surrogate data. Journal of Hydrology. 2023; 621: 129659. doi: 10.1016/j.jhydrol.2023.129659
18. Ehya F, Marbouti Z. Hydrochemistry and contamination of groundwater resources in the Behbahan plain, SW Iran. Environmental Earth Sciences. 2016; 75(6). doi: 10.1007/s12665-016-5320-3
19. Croneborg L, Saito K, Matera M, et al. Digital Elevation Models. World Bank, Washington, DC; 2020.
20. Altafi Dadgar M, Nakhaei M, Porhemmat J, et al. Transient potential groundwater recharge under surface irrigation in semiarid environment: An experimental and numerical study. Hydrological Processes. 2018; 32(25): 3771-3783. doi: 10.1002/hyp.13287
21. Dadgar MA, Nakhaei M, Porhemmat J, et al. Potential groundwater recharge from deep drainage of irrigation water. Science of The Total Environment. 2020; 716: 137105. doi: 10.1016/j.scitotenv.2020.137105
22. Nguyen HH, Peche A, Venohr M. Modelling of sewer exfiltration to groundwater in urban wastewater systems: A critical review. Journal of Hydrology. 2021; 596: 126130. doi: 10.1016/j.jhydrol.2021.126130
23. Das MM, Das Saikia M. Hydrology. Prentice-Hall Of India Pvt. Limited; 2009.
24. Chebanov O, Zadniprovska. Zoning groundwater flooding risks in the cities and urban agglomeration areas of Ukraine. In: Proceedings of the International Union of Geodesy and Geophysics; 2011.
25. Cunnane C. Statistical Distributions for Flood Frequency Analysis. Secretariat of the World Meteorological Organization; 1989.
26. Guerriero L, Ruzza G, Guadagno FM, et al. Flood hazard mapping incorporating multiple probability models. Journal of Hydrology. 2020; 587: 125020. doi: 10.1016/j.jhydrol.2020.125020
27. Hansen A. The Three Extreme Value Distributions: An Introductory Review. Frontiers in Physics. 2020; 8. doi: 10.3389/fphy.2020.604053
28. Solaiman TA. Uncertainty estimation of extreme precipitations under climate change: A non-parametric approach [PhD thesis]. The University of Western Ontario; 2011.
29. Sozer B, Kocaman S, Nefeslioglu HA, et al. Preliminary investigations on flood susceptibility mapping in ankara (turkey) using modified analytical hierarchy process (M-AHP). The International Archives of the Photogrammetry, Remote Sensing and Spatial Information Sciences. 2018; XLII-5: 361-365. doi: 10.5194/isprs-archives-xlii-5-361-2018

30. Elassal M. Geomorphological of hazard maps in ABAH Urban, KSA. Bulletin de la Société de Géographie d'Egypte. 2019; 92(1): 53-75. doi: 10.21608/bsge.2019.90374
31. Darabi H, Choubin B, Rahmati O, et al. Urban flood risk mapping using the GARP and QUEST models: A comparative study of machine learning techniques. Journal of Hydrology. 2019; 569: 142-154. doi: 10.1016/j.jhydrol.2018.12.002
32. Rafiei-Sardooi E, Azareh A, Choubin B, et al. Evaluating urban flood risk using hybrid method of TOPSIS and machine learning. International Journal of Disaster Risk Reduction. 2021; 66: 102614. doi: 10.1016/j.ijdrr.2021.102614
33. Taromideh F, Fazloula R, Choubin B, et al. Urban Flood-Risk Assessment: Integration of Decision-Making and Machine Learning. Sustainability. 2022; 14(8): 4483. doi: 10.3390/su14084483
34. Gaitan S, ten Veldhuis M claire, van de Giesen N. Spatial Distribution of Flood Incidents Along Urban Overland Flow-Paths. Water Resources Management. 2015; 29(9): 3387-3399. doi: 10.1007/s11269-015-1006-y
35. Rincón D, Khan UT, Armenakis C. Flood Risk Mapping Using GIS and Multi-Criteria Analysis: A Greater Toronto Area Case Study. Geosciences. 2018; 8(8): 275. doi: 10.3390/geosciences8080275

Appendix

PDFs

Supposing a number of annual maxima observations $X = \{x_1, x_2, \ldots, x_n\}$:

- Gumbel (Maximum Extreme Value) PDF

$$f(x) = \frac{1}{\sigma} exp(-z - exp(-z)),$$

where $z \equiv \frac{x-\mu}{\sigma}$, σ and μ are scale and location parameters, respectively.

- Frechet (Maximum Extreme Value) PDF

$$f(x) = \frac{\alpha}{\beta}\left(\frac{\beta}{x-\gamma}\right)^{\alpha+1} exp(-\left(\frac{\beta}{x-\gamma}\right)^{\alpha}),$$

where α, β and γ are shape, scale and location parameters, respectively.

- Weibull PDF

$$f(x) = \frac{\alpha}{\beta}\left(\frac{x-\gamma}{\beta}\right)^{\alpha-1} exp(-\left(\frac{x-\gamma}{\beta}\right)^{\alpha}),$$

where α, β and γ are shape, scale and location parameters, respectively.

- Generalized Extreme Value Distribution

$$f(x) = \begin{cases} \frac{1}{\delta} exp(-(1+kz)^{\frac{-1}{k}}), k \neq 0 \\ exp(-exp(-z)), k = 0 \end{cases},$$

where k, σ and μ are shape, scale and location parameters, respectively.